A&A 415, 885–888 (2004)
DOI: 10.1051/0004-6361:20034491

Astronomy & Astrophysics

Star formation rates of distant luminous infrared galaxies derived from Hα and IR luminosities*

H. Flores[1], F. Hammer[1], D. Elbaz[2], C. J. Cesarsky[3], Y. C. Liang[1], D. Fadda[4], and N. Gruel[1]

[1] GEPI, Observatoire de Paris Meudon, 92190 Meudon, France
[2] CEA Saclay – Service d'Astrophysique, Orme des Merisiers, 91191 Gif-sur-Yvette Cedex, France
[3] ESO, Karl-Schwarzschild Straße 2, 85748 Garching bei München, Germany
[4] Instituto de Astrofísica de Canarias (IAC), via Lactea S/N, 38205 La Laguna, Tenerife, Spain

Received 14 March 2003 / Accepted 31 October 2003

Abstract. We present a study of the star formation rate (*SFR*) for a sample of 16 distant galaxies detected by ISOCAM at 15 μm in the CFRS0300+00 and CFRS1400+52 fields. Their high quality and intermediate resolution VLT/FORS spectra have allowed a proper correction of the Balmer emission lines from the underlying absorption. Extinction estimates using the Hβ/Hγ and the Hα/Hβ Balmer decrement are in excellent agreement, providing a robust measurement of the instantaneous *SFR* based on the extinction-corrected Hα luminosity. Star formation has also been estimated exploiting the correlations between IR luminosity and those at MIR and radio wavelengths. Our study shows that the relationship between the two *SFR* estimates follow two distinct regimes: (1) for galaxies with $SFR_{\rm IR}$ below ~100 $M_\odot$/yr, the *SFR* deduced from Hα measurements is a good approximation of the global *SFR* and (2) for galaxies near ULIRG regime. The corrected Hα *SFR* understimated the *SFR* by a factor of 1.5 to 2. Our analyses suggest that heavily extincted regions completely hidden in optical bands (such as those found in Arp 220) contribute less than 20% of the global budget of star formation up to $z = 1$.

Key words. galaxies: formation

1. Introduction

In the last few years, great steps toward a better understanding of the distant Universe have been made using a panchromatic approach. The mid IR windows opened by the camera ISOCAM (Cesarsky et al. 1996) have lead to the identification of the galaxies responsible for the bulk of the infrared background, a population of dusty galaxies that evolves very rapidly in number (Elbaz et al. 1999, 2002). Luminous Infrared Galaxies (LIRGs, $L_{\rm IR} \geq 10^{11}\ L_\odot$) detected by ISO are mainly dusty starbursts (Fadda et al. 2002) with large star formation (>50–100 $M_\odot$/yr) triggered by interactions; ~30–40% of detected galaxies show optical signs of interaction (Flores et al. 1999). Rigopoulou et al. (2000, hereafter R00) using the VLT studied the near IR spectra of a few LIRGs and claimed that the *SFR* measured from IR luminosity (hereafter $SFR_{\rm IR}$) is at least 3 times higher than that based on Hα luminosity (hereafter $SFR_{\rm H\alpha}$). However, this claim is affected by large uncertainties on the $SFR_{\rm H\alpha}$, in the absence of proper extinction correction. Extinction for such heavily dust-shrouded objects is very important, and only accurate estimates of the extinction can confirm the R00 claim. Recently, Hammer et al. (2001) have analyzed intermediate resolution VLT/FORS spectra (R = 3.5 Å at rest) of 3 compact LIRGS at $z \sim 0.6$. They derived accurate fluxes for Balmer emission lines (Hβ, Hγ) after removal of the underlying stellar absorption. Extinction estimates using observed Hβ/Hγ ratios were used to correct Hβ luminosities and derive $SFR_{\rm H\alpha}$ consistent with $SFR_{\rm IR}$. These objects present strong metallic and Balmer absorption lines combined with intense emission lines, which indicate a particularly complex star formation history (Hammer et al. 2001). It is unclear if these properties are shared by the whole galaxy population at intermediate redshifts. Indeed, at $z \geq 0.4$, an important fraction of the galaxy population was identified as Balmer-strong galaxies with emission, in the field (Hammer et al. 1997) and in galaxy clusters (Poggianti et al. 1999).

Here we present a preliminary study of 16 LIRGs out of a sample of 90 observed at VLT and CFHT. The data are described in Sect. 2. Section 3 summarizes the different techniques used for the data analysis. The determination of the *SFR* is discussed in Sects. 4 and 5. Throughout this paper we adopt $H_0 = 50$ km s^{-1} Mpc^{-1} and $q_0 = 0.5$ ($\Omega_M = 1, \Omega_\Lambda = 0$).

2. Observations and sample selection

Deep MIR data were obtained in a region of 13×13 sq. arcmin centered on the CFRS0300+00 field, using ISOCAM broad-band filters LW3 (12–18 μm, centered at 14.3 μm) and LW2 (5–8 μm, centered at 6.75 μm) for a total integration time per

Send offprint requests to: H. Flores,
e-mail: hector.flores@obspm.fr

sky position of 23 and 15 min, respectively. The reduction of IR data was done using the standard method described by Fadda et al. (2001), resulting in a catalog of detected sources which will be published in a subsequent paper.

Among the 40 LIRGs galaxies with known redshift (from the Canada France Redshift Survey, Hammer et al. 1995) we have randomly selected 14 galaxies which were observed together using the VLT/FORS2/MXU (runs 66.A-0599(A), 68.A-0298(A)) and 2 additional objects observed with the CFHT/MOS (run 98IF65A). The 8 distant LIRGs ($z > 0.6$) were pre-selected to avoid contamination of their near IR redshifted Hα line by strong OH sky emission. The sample is representative of LIRGs in the CFRS0300+00 field. Optical VLT observations were done in service mode during periods 66 and 68 using two differents FORS2 set-ups (R600 and I600 grisms, 3 h each, $R \sim 1300$) with a slit width of 1.5 arcsec. CFHT data were obtained in two different runs in 1998 and 2000, using the standard MOS setup (R300 grism and 1.5 arcsec slit, 4 h, $R = 660$). Near IR spectra of four galaxies were collected in runs 66.A-0599(A) and 69.B-0301(A) with the infrared spectrometer VLT/ISAAC. For the near IR observations we used the medium resolution grating $R_s \sim 3000$ and a 2″ slit, for a total of 1 h of integration time nodding along the slit (ABBA configuration). Targets were first acquired using a reference star at a distance of 1′, with a 1–2 min exposure in the *J*s-band. For four objects, we used VLT/ISAAC archive data (Program 63.O-0270(A)). These galaxies were observed using the same instrumental setup. Data reduction and extraction of optical and near-IR spectra were performed using a set of IRAF procedures developed by our team, which allowed us to reconstruct simultaneously the spectra and the sky counts of the objects.

3. Data analysis procedure

Figure 1 shows the median optical (VLT/FORS) and the near IR VLT spectra (VLT/ISAAC) of the 8 distant LIRGs. The spectra were flux-calibrated using standard stars for both optical and near IR spectra. Broadband filter images (*V* to *I* bands for FORS spectra, *J* band for ISAAC spectra) were used to compute the spectroscopic aperture corrections. To check the validity of the relative aperture corrections, we produced best fit models of both spectra and photometry using population synthesis models (Bruzual & Charlot 1993) appropriately corrected for extinction. This procedure has provided an independant test of the spectral calibration and of possible errors in aperture corrections. The uncertainty related to our derived calibration is well below 15%. The underlying Balmer absorption lines were estimated after synthetizing the galaxy continuum from 3730 Å to 5000 Å, including major metallic lines and the high order absorption Balmer lines unaffected by emission. Synthetic spectra were produced from combinations of 4 stars from *B* to *K* type, selected from Jacoby et al. (1984), appropriately chosen to best fit the continuum and absorption line spectra (see details in Hammer et al. 2001; Gruel Ph.D. Thesis 2002).

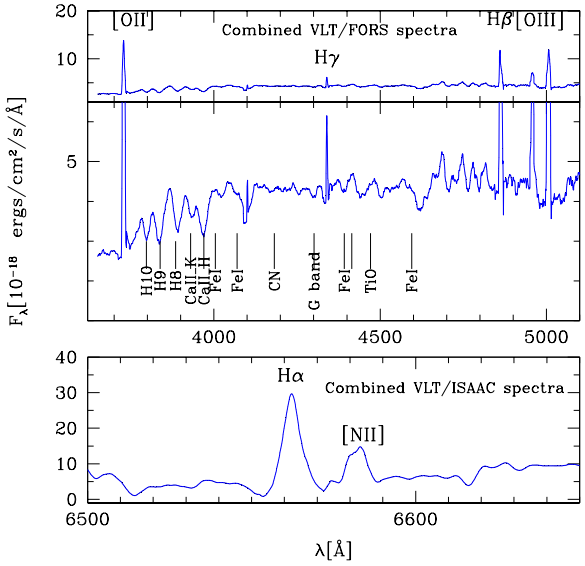

Fig. 1. Combined VLT FORS+ISAAC spectra, after masking sky emission lines, and smoothing the continuum of both galaxies (see Hammer et al. 2001; Gruel et al., in preparation). Zooms in the center shows details of our spectra (*S/N* > 5 per resolution element in the continuum), including the underlying Balmer absorption. Lower panel shows combined near IR spectra.

4. Extinction and *SFR* from Hα, Hβ and Hγ Balmer emission lines

Median resolution VLT spectra (FORS+ISAAC) allowed us to measure three Balmer emission lines (Hγ, Hβ and Hα) for distant LIRGs. Extinctions were derived from both the Hβ/Hγ and the Hα/Hβ Balmer ratios using a standard extinction law (Fitzpatrick 1999). Table 1 lists the corresponding A_V and the associated error bars. Relative errors due to *S/N* and data analysis methodology have been quadratically added, and hence the final error bars correspond to more than a 1σ error. The extinction factor of LIRGs averages to $A_V \sim 2.8$ at $z \sim 0.7$, a value much larger than $A_V = 1.12$ obtained by Kennicutt (1992) for normal spiral galaxies or $A_V = 0.57$ derived by Gallagher et al. (1989) for irregular galaxies. Figure 2 shows the excellent correlation between extinction estimates from the Hβ/Hγ and the Hα/Hβ ratios. *SFR* were calculated using the extinction-corrected Hα line (Hβ in the case of galaxy 03.0495) integrated flux following the methods of Kennicutt (1998). The correlation displayed in Fig. 2a is valid over a wide range of redshifts and luminosity. We give in this paper the most accurate evaluation of *SFR* of starbursts and LIRGS done up to now on the basis of Balmer lines. Having reached the limits of the method, we evaluate the validity of its application in ascertaining actual *SFR*s in dusty galaxies.

5. *SFR* derived from multi-wavelength correlations

A major fraction of the ionising photons related to star formation was reprocessed by dust in dust-enshrouded galaxies such as the LIRGs studied here. The IR luminosity (8–1000 μm) may also provide a good estimate of the *SFR*. We estimated

Table 1. Extinctions and *SFR* of distant LIRGs and nearby galaxies detected by ISO.

CFRS...	z	I	M_B	$A_v[H\beta/H\gamma]^a$	$A_v[H\alpha/H\beta]^a$	SFR^b_{2800}	$Flux^c_{H\alpha}$	Ap^d	$SFR^e_{H\alpha}$	SFR^k_{IR}	SFR^l_{IR}
3.0422	0.7154	21.21	−21.45	$2.73^{3.88}_{1.89}$	$3.11^{4.06}_{1.33}$	4.82	26.6 ± 13.9^g	1.5	$148.8^{+200.4}_{-119.1}$	218.1 ± 58.0	
3.0523	0.6530	21.31	−21.19	$2.09^{2.33}_{1.98}$	$2.29^{2.37}_{2.19}$	4.55	70.0 ± 5.0^h	1.0	$101.5^{+7.9}_{-8.2}$	108.2 ± 30.2	123.0
3.0570^j	0.6480	22.07	−20.38	$1.73^{2.25}_{1.29}$	$2.03^{2.53}_{1.33}$	1.87	22.1 ± 5.8^g	1.4	$34.8^{+20.3}_{-16.2}$	35.9 ± 19.2	
3.1242^j	0.7687	21.69	−21.21	$2.83^{4.24}_{2.47}$	$3.02^{3.24}_{2.65}$	6.11	31.0 ± 9.4^g	1.0	$124.3^{+27.6}_{-35.4}$	110.3 ± 66.4	
3.1309	0.6170	20.62	−21.76	$2.57^{3.28}_{1.89}$	$2.37^{2.70}_{1.97}$	7.90	42.1 ± 7.0^h	1.3	$75.8^{+26.1}_{-23.0}$	192.6 ± 30.0	279.5
3.1349	0.6155	20.87	−21.42	$2.56^{3.11}_{2.40}$	$2.79^{2.79}_{2.79}$	4.39	25.5 ± 2.4^g	2.2	$113.2^{+0.9}_{-0.1}$	144.0 ± 34.5	
3.1540	0.6890	21.04	−21.52	$3.02^{3.80}_{2.76}$	$3.10^{3.22}_{2.93}$	4.11	47.0 ± 8.0^h	1.0	$160.1^{+19.1}_{-22.4}$	266.4 ± 53.6	282.7
3.9003	0.6189	20.77	−21.51	$2.41^{5.86}_{0.68}$	$2.44^{2.70}_{2.07}$	4.41	48.0 ± 12.3^g	1.0	$71.5^{+18.3}_{-20.7}$	75.7 ± 24.7	
3.0365	0.2180	19.19	−20.09	–	$1.75^{1.99}_{1.57}$	0.38	65.1 ± 6.0^i	2.6	$14.7^{+3.5}_{-2.2}$	13.2 ± 1.8	
3.0495	0.2612	19.43	−20.30	$1.37^{2.54}_{0.34}$	–	0.37	7.3 ± 0.4^f	2.7	$26.0^{+69.6}_{-16.5}$	14.6 ± 3.8	38.9
3.0828	0.3307	22.44	−18.25	$1.14^{3.15}_{0.02}$	$1.84^{2.06}_{1.66}$	0.19	3.7 ± 0.3^h	3.8	$3.2^{+0.5}_{-0.7}$	27.5 ± 7.7	
3.0949	0.0327	17.48	−17.55	–	$3.51^{6.08}_{2.35}$	0.05	203.0 ± 13.0^h	2.6	$4.7^{+42.9}_{-3.1}$	0.9 ± 0.1	0.7
3.1014	0.1961	18.42	−20.87	–	$1.86^{1.93}_{1.81}$	1.25	35.0 ± 5.0^h	4.6	$12.4^{+0.7}_{-0.6}$	7.1 ± 1.9	
3.1299	0.1760	18.59	−20.49	–	$0.96^{1.01}_{0.89}$	0.99	82.0 ± 10.0^i	2.5	$5.6^{+0.3}_{-0.4}$	15.4 ± 1.5	
3.1311	0.1800	19.56	−19.41	–	$2.58^{2.73}_{2.45}$	0.31	67.6 ± 4.0^h	1.8	$15.0^{+2.2}_{-1.7}$	5.5 ± 1.3	9.7
14.1117^j	0.1900	20.79	−18.98	–	$0.41^{0.67}_{0.20}$	0.60	21.0 ± 1.5^i	5.4	$2.2^{+0.6}_{-0.4}$	3.3 ± 1.5	

– In Cols. (3) and (4) I band magnitude and B absolute magnitude are *AB* system magnitudes.
[a] Extinction in magnitude at 5500 Å, including the lower and upper value. [b] *SFR* in $M_\odot$/yr from M_{2800} absolute magnitude. [c] Hα integrated flux in units of 10^{-17} [ergs/cm^2/s/Å]. [d] Aperture correction of Hα emission line. [e] *SFR* in $M_\odot$/yr after correction for aperture and errorbars. [f] Derived from Hβ flux measured in the VLT spectra. [g] Recovered from VLT/ISAAC archive. [h] VLT, FORS or ISAAC spectra. [i] CFHT/MOS spectra. [j] 15 μm no-secure source catalog. [k] IR *SFR* deducted from MIR relationship in $M_\odot$/yr. [l] IR *SFR* deducted from radio-IR relationship in $M_\odot$/yr.

the *SFR* using a set of SED templates from the STARDUST II model (Chanial et al., in preparation) and the relationship found by Elbaz et al. (2002) between the MIR and the IR luminosity. For a few objects detected at radio wavelengths we have also derived the IR luminosity from the radio-FIR correlation (see Condon 1992). All three methods produce results consistent within the error bars which are dominated by the uncertainties in the MIR photometry and the scatter of MIR (or radio)- IR relationship. *SFR* has been computed assuming the formula of Kennicutt (1998), and allowing a direct comparison with our derivation of the *SFR* from Balmer emission lines, since both calculations assumed a Salpeter (1995) IMF with mass limits from 0.1 to 100 $M_\odot$.

6. Discussion and conclusions

Extinction affects potentially a large fraction of cosmological sources and their consequences have been the subject of long debate in observational cosmology. Here, we study a representative sample of dust-enshrouded starbursts, which, at moderate redshifts, can be extensively studied by spectroscopy, at MIR and at radio wavelengths. We have compared the instantaneous *SFR* related to the optical nebular emission ($SFR_{H\alpha}$) to the *SFR* estimated from the MIR emission measured by ISO , and, when available, from the radio emission. These two methods give compatible results, which we denote by (SFR_{IR}). Hα luminosities have been properly corrected for: (1) extinction (using Balmer decrement ratio); (2) absorption line contamination (using moderate resolution spectroscopy) and (3) aperture (using photometric measurements). Aperture correction can lead to major errors. It assumes that the fraction of the emission line light sampled by the slit equals that of the continuum light derived from broad band photometry, which could be wrong. However, our extinction estimate from the Hβ/Hγ ratio does not depend on such assumptions and agrees well with our estimate from the Hα/Hβ ratio. Moreover, for the 8 distant galaxies, the aperture correction is generally close to 1, and so we believe that uncertainties related to aperture correction are marginal. IR luminosities have been estimated by (1) using the correlation between MIR and far-IR luminosities and (2) using the correlation between radio and far-IR luminosities. A good agreement is found between the two methods. Despite the large error bars on individual *SFR*s, we find a remarquable trend in the relationship between the two *SFR* estimates: (1) for starbursts with SFR_{IR} below 90–130 $M_\odot$/yr, *SFR* estimates based on Hα luminosities, properly corrected, agree well with SFR_{IR}, in agreement with analyses of local galaxies with low *SFR*s (Buat et al. 2002; Rosa-Gonzalez et al. 2002); (2) at larger IR luminosities, Hα emission lines underestimate the *SFR* by factors up to 2.5 at $SFR_{IR} = 250\ M_\odot$/yr; (3) few objects show properties discrepant from the empirical relationship between $SFR_{H\alpha}$ and SFR_{IR} which could be due to their individual star formation history: for example, if the star formation was rapidly decreasing (increasing), one would expect SFR_{IR} larger (smaller) than $SFR_{H\alpha}$. Our result is in excellent agreement with the recent study of the IRAS sources detected by the SDSS (Hopkins et al. 2003, see their Fig. 15) in the local universe. However it substantially differs from that of Franceschini et al (2003, hereafter F03), who have

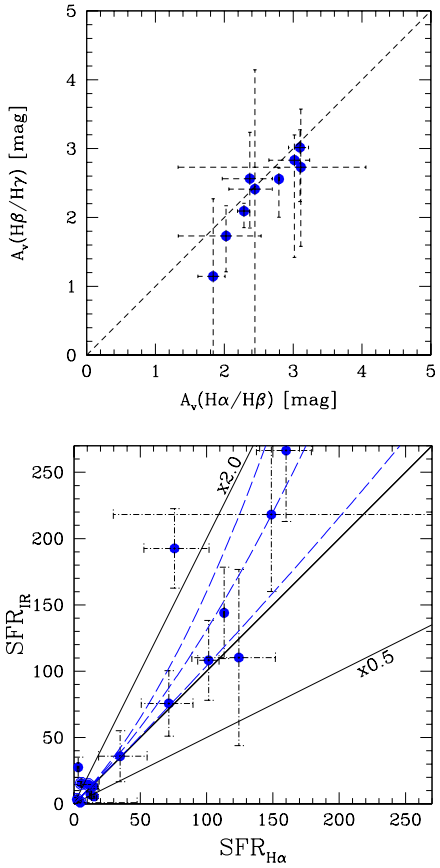

Fig. 2. a) *Upper panel:* this plot shows the strong correlation that exists between the extinction estimated using the two differents Balmer ratios (Hβ/Hγ and Hα/Hβ). **b)** *Bottom panel:* comparison of the two *SFR*s, using MIR luminosities and Balmer emission line luminosities. Full line represents $SFR_{\rm IR} = (2\text{–}1\text{–}0.5) \times SFR_{\rm H_\alpha}$. The dashed-line represents a polynomial (best) fit to the points ($SFR_{\rm IR} = SFR_{\rm H\alpha} \times (1 + a \times SFR_{\rm H\alpha})$, where $a = 3.11^{6.0}_{0.4} \times 10^{-3}$). $SFR_{\rm H\alpha}$ underestimates the global *SFR* for values larger than ∼100 $M_\odot$/yr.

studied similar sources in the HDFS. In F03, Fig. 8, IR and Hα estimates of the *SFR* are similar for LIRGs and ULIRGs, while for most of the less luminous IR galaxies, infrared observations provide larger values of the *SFR*s. Into the above results are somewhat in contradiction our and the Hopkins et al. studies. F03's Table 5 displays extinction corrected $SFR_{\rm H\alpha}$ values for 11 objects. For 7 of them, they have estimated dust extinction from the stellar continuum on the basis of the rest-frame $V - K$ colors or on the comparison between Hα and rest-frame 2800AA fluxes; it is generally believed that the continuum can only provide gross estimates of the gas extinction, because it is strongly affected by the various and complex star formation histories. For the 4 remaining objects (HDFS25, 27, 53 and 55), the discrepancy might be related to the fact that F03 have not corrected Hβ fluxes for underlying absorption, leading to a systematic underestimate of Hβ emission flux. Moreover 2 of these objects (HDFS25, 55) present a low *S/N* for the Hα line (see R00, Fig. 1).

Using both *SFR*s, we have estimated an empirical polynomial relationship $SFR_{\rm IR} = SFR_{\rm H\alpha} \times (A \times SFR_{\rm H\alpha} + 1)$, where $A = 3.11^{6.0}_{0.4} \times 10^{-3}$ (which fits at best the points in Fig. 2b, weighted according to the error bars). Applying our empirical relationship to the $L_{\rm IR}$ estimated by Flores et al. (1999) on field galaxies, one can derive in principle the Hα luminosity density corresponding to the IR luminosity density at $z \leq 1$ (note that this result is insensitive to a change of cosmological constants). The Hα star formation density corresponds to 83% to 89% of the IR star formation density, for the Flores et al. lower and upper limit, respectively. This suggest that galaxies that dominate the cosmic star formation density at $z \leq 1$ are not ULIRGs, but correspond to the much more abundant population of LIRGs and starbursts. To determine the *SFR*, MIR fluxes which can be measured rapidly by satellites (ISO, SIRTF) give, at least for the intrinsically bright IR galaxies, more accurate estimates than cumbersome optical and NIR spectroscopy. However, the detailed spectra provide useful information on metal abundances and on the evolutionary history of the galaxies, as we will show in subsequent papers.

Acknowledgements. We thank Rafael Guzmán for enlightening discussions which greatly contributed to improve our paper.

References

Buat, V., Boselli, A., & Gavazzi, G. 2002, A&A, 383, 801
Cesarsky, C. J., Abergel, A., Agnese, P., et al. 1996, A&A, 315, 32
Elbaz, D., Cesarsky, C. J., Fadda, D., et al. 1999, A&A, 351, L37
Elbaz, D., Cesarsky, C. J., Chanial, P., et al. 2002, A&A, 384, 848
Fadda, D., Elbaz, D., Duc, P.-A., et al. 2000, A&A, 361, 827
Fadda, D., Flores, H., Hasinger, G., et al. 2002, A&A, 383, 838
Fitzpatrick, E. 1999, PASP, 111, 63
Flores, H., Hammer, F., Thuan, T. X., et al. 1999, ApJ, 517, 148
Franceschini, A. 2003, A&A, 403, 501
Gallagher, J., Hunter, D. A., Bushouse, H. 1989, AJ, 98, 806
Hammer, F., Flores, H., Lilly, S. J., et al. 1997, ApJ, 481, 49
Hammer, F., Cruel, N., Thuan, T. X., et al. 2001, ApJ, 550, 570
Hopkins, A. M., et al. 2003 [astro-ph/0306621]
Jacoby, G. H, Hunter, D. A., & Christian, C. A. 1984, ApJS, 56, 257
Kennicutt, R. C. 1998, Ann. rev. Astr. Ap., 36, 189
Kennicutt, R. C. 1992, ApJ, 388, 310
Poggianti, B. M., Smail, I., Dressler, A., et al. 1999, ApJ, 518, 576
Rigopoulou, D., Franceschini, A., Aussel, H., et al. 2000, ApJ, 537, 85
Rosa-González, D., Terlevich, E., & Terlevich, R. 2002, MNRAS, 332, 283